Computation of Direct Sensitivities of Spatial Multibody Systems with Joint Friction

Adwait Verulkar *
Terramechanics, Multibody and
Vehicle Systems Laboratory
Department of Mechanical Engineering
Virginia Polytechnic Institute and State University
Blacksburg, Virginia 24061
Email: adwaitverulkar@vt.edu

Corina Sandu
Terramechanics, Multibody and
Vehicle Systems Laboratory
Department of Mechanical Engineering
Virginia Polytechnic Institute and State University
Blacksburg, Virginia 24061
Email: csandu@vt.edu

Daniel Dopico
Laboratorio de Ingeniería Mecánica
Department of Naval and Industrial Engineering
University of A Coruña
A Coruña, Spain 15001
Email: ddopico@udc.es

Adrian Sandu
Computational Science Laboratory
Department of Computer Science
Virginia Polytechnic Institute and State University
Blacksburg, Virginia 24061
Email: asandu7@vt.edu

Friction exists in most mechanical systems and may have a major influence on the dynamic performance of the system. The incorporation of friction in dynamic systems has been a subject of active research for several years owing to its high non-linearity and its dependence on several parameters. Consequently, optimization of dynamic systems with friction becomes a challenging task. Gradient-based optimization of dynamical systems is a prominent technique for optimal design and requires the computation of model sensitivities with respect to the design parameters. The novel contribution of this paper is the derivation of the analytical methodology for the computation of direct sensitivities for smooth multibody systems with joint friction using the Lagrangian index-1 formulation. System dynamics have been computed using two different friction models; the Brown and McPhee, and the Gonthier et al. model. The methodology proposed to obtain model sensitivities has also been validated using the complex finite difference method. A case study has been conducted on a spatial multibody system to observe the effect of friction on the dynamics and model sensitivities, compare sensitivities with respect to different parameters and demonstrate the numerical and validation aspects. Since design parameters can have very different magnitudes and units, the sensitivities have been scaled with the parameters for comparison. Finally, a discussion has been presented on the interpretation of the case study results. Due to incorporation of joint friction, 'jumps' or discontinuities are observed in the model sensitivities akin to those observed for hybrid dynamical systems.

*Address all correspondence to this author.

Nomenclature

nb Number of bodies in the system.

n Number of generalized coordinates. $7nb$ for reference point coordinates with Euler parameters.

$\mathbf{q} \in \mathbb{R}^n$ Vector of generalized coordinates.

$\boldsymbol{\lambda} \in \mathbb{R}^m$ Vector of Lagrange multipliers.

$\boldsymbol{\rho} \in \mathbb{R}^p$ Vector of system parameters $[\rho_1, \ldots, \rho_p]^{\mathrm{T}}$.

$\mathbf{y}_{\mathbf{x}}$ Jacobian formed by partial derivatives $\frac{\partial \mathbf{y}}{\partial \mathbf{x}}$.

$\dot{x}, \ddot{x}$ Time derivatives $\frac{\mathrm{d}x}{\mathrm{d}t}$ and $\frac{\mathrm{d}^2x}{\mathrm{d}t^2}$ respectively.

$\boldsymbol{\Phi}(\mathbf{q}, \boldsymbol{\rho}) \in \mathbb{R}^m$ Vector of m holonomic constraints.

$\boldsymbol{\Phi}_{\mathbf{q}} \in \mathbb{R}^{m \times n}$ The constraint vector Jacobian.

$\mathbf{M}(\mathbf{q}, \boldsymbol{\rho}) \in \mathbb{R}^{n \times n}$ Mass matrix.

$\mathbf{Q}(\mathbf{q}, \dot{\mathbf{q}}, \boldsymbol{\rho}) \in \mathbb{R}^n$ Vector of external generalized forces and torques.

$\mathbf{Q}^{Af}(\mathbf{q}, \dot{\mathbf{q}}, \boldsymbol{\lambda}, \boldsymbol{\rho}) \in \mathbb{R}^n$ Vector of generalized frictional forces.

v Magnitude of relative sliding velocity.

v_t Magnitude of transition velocity.

$\boldsymbol{\mu}$ $[\mu_d, \quad \mu_s]^{\mathrm{T}}$, where μ_d and μ_s are coefficients of dynamic and static friction respectively.

$S(v, v_t, \boldsymbol{\mu})$ Brown and McPhee friction coefficient.

$F_n(\mathbf{q}, \boldsymbol{\lambda}, \boldsymbol{\rho})$ Magnitude of normal force of contact.

F_f Magnitude of friction force.

$\mathbf{R}$ Residual of constrained equations of motion.

$\mathbf{r}_i \in \mathbb{R}^3$ Global position vector for the ith body-fixed reference frame.

$\mathbf{u}_i$ Axis of rotation which forms the basis for the Euler parameters for body i. Any spatial rotation can be represented as a single rotation about this axis.

χ_i Angle of rotation about $\mathbf{u}$ for body i. Conventionally considered positive counter-clockwise.

$\mathbf{p}_i \in \mathbb{R}^4$ Euler parameter vector for i^{th} body-fixed reference frame given by $[e_0 \quad \mathbf{e}^{\mathrm{T}}]^{\mathrm{T}}$ where $e_0 = \cos(\chi/2)$, and $\mathbf{e} = \sin(\chi/2)\mathbf{u}$.

$\mathbf{s}'_i \in \mathbb{R}^3$ Position vector for joint location in the local i^{th} body-fixed reference frame.

$\mathbf{u}_{ij} \in \mathbb{R}^3$ Relative velocity of sliding between bodies i and j at joint surface.

$\mathbf{A}_i \in \mathbb{R}^{3\times 3}$ Euler parameter rotation matrix representing a transformation from i^{th} body-fixed coordinate system to global coordinate system. $\mathbf{A}(\mathbf{p}) = (e_0^2 - \mathbf{e}^{\mathrm{T}}\mathbf{e})\mathbf{I} + 2\mathbf{e}\mathbf{e}^{\mathrm{T}} + 2e_0\tilde{\mathbf{e}}$.

$\mathbf{B}_i \in \mathbb{R}^{3\times 4}$ $2\left[(e_0\mathbf{I} + \tilde{\mathbf{e}})\,\mathbf{s}'_i \quad \mathbf{e}\mathbf{s}'^{\mathrm{T}}_i - (e_0\mathbf{I} + \tilde{\mathbf{e}})\,\tilde{\mathbf{s}'_i}\right]$.

$\mathbf{E}_i \in \mathbb{R}^{3\times 4}$ $[-\mathbf{e} \quad \tilde{\mathbf{e}} + e_0\mathbf{I}]$.

$\mathbf{G}_i \in \mathbb{R}^{3\times 4}$ $[-\mathbf{e} \quad -\tilde{\mathbf{e}} + e_0\mathbf{I}]$.

$\mathbf{C}_i \in \mathbb{R}^{3\times 3}$ Rotation matrix representing a transformation from the joint definition frame to the ith body-fixed reference frame.

h Time step.

ε Convergence error.

i Iteration index.

δ Convergence error tolerance.

$\aleph$ Maximum convergence iterations.

m Mass of block.

g Acceleration due to gravity.

k Spring constant.

σ_0 Bristle stiffness.

σ_1 Bristle damping.

σ_2 Coefficient of viscous friction.

τ_{dw} Dwell time-constant.

v_ε Numerical tolerance in velocity for body at rest.

v_s Stribeck effect velocity (equivalent to v_t).

1 Introduction

In recent years, multibody dynamics has evolved into a crucial tool of synthesis and design of mechanical systems, having applications in a myriad of fields such as automotive, aerospace, robotics and industrial automation, control, and parameter estimation. Optimization of such systems requires state-of-the-art gradient based techniques which fundamentally require sensitivity analysis with respect to their design parameters. The techniques deployed most frequently are the direct sensitivity approach and the adjoint sensitivity approach. The adjoint sensitivity approach was first presented by Haug and Arora [1] in 1978 and this approach was extended towards constrained dynamic systems in 1984 by Haug et al. [2]. This approach is more suitable if the number of parameters 'p' is relatively large while the number of objective functions 'o' is small. In this approach, the computation of individual sensitivities is not required to compute the gradient of the objective function, which is where the efficiency of this approach comes from. The direct sensitivity approach for constrained dynamic systems was developed by Krishnaswami and Bhatti [3]. The direct sensitivity analysis approach is preferred if the number of parameters 'p' is relatively small [4] and the number of objective functions 'o' is large. As the number of parameters grows, this methodology becomes computationally expensive.

Over the years, several sensitivity analysis methodologies have been developed. Haug [5] developed the methodology using index-3 and index-1 formulations. Chang and Nikravesh [6] added Baumgarte stabilization [7] to dynamic systems to prevent constraint violation. Pagalday and Avello [8] performed sensitivity analysis using Augmented Lagrangian Penalty Formulation. Direct and adjoint sensitivity analysis using Ordinary Differential Equation (ODE) formulation was presented by Dopico et al. [9]. This formulation enables the use of standard well-established integration schemes, like 4th-order Runge-Kutta as used by Flores et al. [10], to be used for the solution of dynamics and sensitivities. Zhang and Sandu [11] have developed a library for computationally efficient integration of ODEs.

In the past few years sensitivity analysis approach has been developed for hybrid systems, or systems that have piece-wise continuous velocity trajectories. Corner et al. [12] developed the direct sensitivity analysis approach for such systems. These discontinuities might be caused by events such as impacts which results in a sudden change of constraints. Most recently, Corner et al. [13] extended their work on hybrid systems and presented a methodology for adjoint sensitivity analysis of hybrid systems. Among other applications, sensitivity analysis can also be employed for parameter estimation. Blanchard et al. presented his work on parameter estimation for mechanical systems with uncertain parameters using polynomial chaos representation of uncertainty [14–16].

The current state-of-art research in the field of multibody dynamics is focused on topics like modeling and simulation of hybrid dynamic systems, flexible multibody systems, bio-mechanical systems and rehabilitation, and modeling of systems with non-ideal joints. There might be a variety of reasons that lead to the deviation of the joint performance from the ideal behavior. These imperfections may include things such as joint clearances [17, 18], which may be unintentional due to wear or intentional due to backlash or to provide clearance for lubrication and leads to a deviation from the ideal joint performance due to viscous drag [10]. The focus of this article is on modeling and sensitivity analysis of systems where the joint friction forces cannot be neglected. Although research on multibody systems with friction is ongoing since quite some time, spatial multibody formulations with joint friction were developed very recently. There has been some work on this topic in the late 1980s in the form a series of papers where the theory of constraint addition and deletion was presented [19–21]. Over the years, there was progress made on this topic [22, 23] but efficient and generalized formulations for joint friction were not described. The recent developments by Pennestri et al. [24] which presents the formulation for multibody dynamics of planar systems with Dahl friction and Blumentals et al. [25] have shown a lot of promise. Other recent works include the papers by Wojtyra, and Harlecki and Urbaś [26, 27].

This paper studies the sensitivity analysis of multibody systems with joint friction. Such systems require the compu-

tation of the joint normal forces, which essentially are functions of the Lagrange multipliers. Hence, it is very natural to model such systems using the Lagrangian DAE formulations. The novel contribution of this work is to develop and validate the analytical methodology for computation of direct sensitivities of smooth multibody systems with joint friction. This work builds on the multibody formulation presented by Haug [28] that incorporates joint friction using the Brown-McPhee friction model [29]. The results presented in this study not only include the methodology for sensitivity analysis using Brown-McPhee friction model [30] but also incorporates a more versatile dynamic friction model given by Gonthier et al. [31]. Both of these models are capable of emulating behaviors of stiction (static friction), sliding friction, viscous drag, and Stribeck effects. Additionally, a brief review of the friction models relevant for dynamical systems has been presented which includes a discussion on the selection criteria of a model for sensitivity analysis. The Lagrangian index-1 formulation has been used to develop a tangent space model for computation of multibody system sensitivities through direct differentiation. For validation of this analytical methodology, sensitivities have also been computed using complex Finite Difference Method (FDM) and compared against those obtained through the methodology. Typically, index-1 Lagrangian formulations pose some numerical difficulties during forward dynamics computation due to the high numerical stiffness of the formulation. These drawbacks were addressed by Zhu et al. [32] by using penalty formulation for adjoint sensitivities. Penalty formulations are also well suited for redundant constraints and kinematic bifurcations, which are common issues in spatial mechanisms. A better option than the penalty approach is the ALI3-P formulation derived by Dopico et al. [33]. Another valid option is the ODE formulation [9] which is also suited to redundant constraints. However, in this study suitable implicit integration schemes have been implemented to mitigate the stiffness associated with index-1 Lagrangian formulations. Due to the incorporation of friction, Lagrange multipliers appear on both sides of the dynamic equations of motion. To solve such equations, a fixed-point iteration scheme has been implemented in the study and its convergence has been demonstrated. All the numerical results shown in this work have been obtained through the implementation of the proposed methodology on a spatial mechanism. The effect of friction on dynamics and model sensitivities has been studied. An interesting result of incorporating joint friction is that, although the dynamic model is continuous, abrupt changes in model sensitivities can be observed during transition phases of friction (static to dynamic and vice versa). This is similar to the sensitivity 'jump' observed for hybrid dynamical systems [12].

2 A Review of Friction Models for Multibody Systems

Substantial work has been done on the development of friction models over the last 5 centuries [34], yet not a single mathematical model has been developed that can conclusively model this phenomenon [35]. This can be attributed to its dependence on a large number and variety of parameters. The most significant of these being the magnitude of the normal force acting between surfaces in contact, surface irregularities or roughness, and the tendency of those surfaces to adhere to each other. Other parameters such as sliding speed, surface temperature, humidity and materials also play key roles. Surface temperature, for example, plays a major role in braking systems, and is the dominant factor contributing to the brake fading phenomenon commonly seen in automotive racing. Not only does friction depend on the physical parameters of the system, but also depends on the nature of the contact itself. Friction for sliding contacts is very different than friction for rolling contacts. Lubrication also plays a significant part, as it fundamentally alters the nature of friction between two surfaces.

Berger points out very acutely in his review paper [35] that the complexity of the friction model being used should be in accordance with that of the dynamic model of the system. These two models cannot be chosen independent of each other. Choosing a simplistic friction model that is incapable of using most of the dynamic states would eventually lead inaccurate system models. Broadly speaking, friction is modeled either as a continuous time phenomenon which is generally used in mechanics related problems or as a discrete time phenomenon which is typically used in control related problems. For effective control of mechanical systems, it becomes necessary to estimate friction in the system model. Hence, it is required that the friction models used for control applications be easy to implement within the system dynamics. Ideally, it is preferred if the friction model is continuous across the friction regimes (sticking and sliding) and the model is non-stiff, differentiable and integrable. Moreover, the parameters used in the model should have physical significance and be easy to measure/estimate. If the friction model is continuous in time and has Lipschitz continuity in the systems states, it is possible to implement it within the system dynamics using the theory of hybrid systems [36]. These criteria are also useful for selecting appropriate friction model for sensitivity analysis.

For nearly two centuries, friction was modeled using the formulation proposed by Coulomb in 1785. The model gave a range of values for zero relative velocity and a constant value for non-zero relative velocities. The sign of the friction was decided based on the fact that friction always acts in a direction so as to resist relative motion. In 1968, Dahl [37], observed that small amplitude input forces also faced a reaction by elastic restoring forces. Dahl theorized that the macroscopic friction we observe in real life is just a manifestation if the microscopic interactions and bonds formed between two contact surfaces. Unlike the Coulomb friction model, Dahl thought of friction as a stress-strain like behavior in material deformation tests. This idea was conveyed by Dahl by proposing a model that assumes two bodies making contact through elastic bristles, similar to a brush. The transition from static to kinetic friction is similar to the transition from elastic to plastic deformation in ductile materials. This analogy works perfectly, as explained below:

1. The static friction regime can be related to elastic deformation of the bonds and hence upon removal of the applied force, the bonds return to their original state.
2. The transition regime from static to dynamic friction can be thought of as a plastic deformation, where there is some hysteresis and the bonds do not return exactly to their original states.
3. Finally the dynamic friction regime is analogous to fracture of the material, since the bonds that are responsible for friction have eventually broken as the applied load is higher than the amount which can be supported by the bonds. This regime is when there is a constant shearing of the friction bonds.

There are multibody formulations which have incorporated the Dahl friction model [24]. Later, improvements were made to this model by Wit et al. [38] in 1995 as several models started to emphasize the importance of velocity effects, especially in systems involving lubricated surfaces. There were two prominent limitations to the Dahl model namely, it was a purely displacement based model and it did not account for the fact that the load required to cause initial displacement of a body is always higher than that required to sustain motion. Wit et al. model, which was created within a research collaboration between the Lund Institute of Technology (Sweden) and the Laboratoire d'Automatique de Grenoble (France), incorporated many behaviors of friction observed in experiments. The friction model, that is more commonly known as *LuGre* model is a very versatile model capable of simulating the velocity and acceleration dependence of sliding friction, hysterisis effects and pre-slip displacements. LuGre model also reproduces the Stribeck effect, which is a non-linear dependence of friction on the relative velocity of the sliding surfaces. For a finite velocity regime, the surface friction decreases with an increase in the sliding velocity. Beyond a certain threshold however, friction starts increasing if the sliding velocity keeps growing larger. This accuracy of the LuGre model however, comes at the cost of the model complexity, as this is a 6 parameter model. Despite this drawback, the LuGre model for friction is widely accepted in the controls community as it is very suitable for applications requiring accurate macroscopic friction behavior but are not concerned with the finer details of interface response. Other models suitable for control of dynamical systems are the Armstrong-Hélouvry model [39]. This model is a predecessor of the LuGre model and it introduced temporal dependency of friction and the Stribeck effect. However, the pre-sliding displacement phenomenon is described by a separate equation. Thus, it is required to introduce a mechanism in the simulation to switch between the two equations, one for sliding and one for stiction. The model is 7 parameter model, but due to the switching requirement an 8th parameter might be required. The Bliman-Sorine model [40,41], which is also based on the Dahl friction model, has subtle differences when compared to the LuGre model. The Stribeck effect in Bliman-Sorine model is not the same as that observed in experimentation. Moreover, the model has an oscillatory response in the stiction regime. Gonthier et al. [31] made further modifications to the LuGre model and presented a new model in 2004. The authors added a dwell-time dependency to the LuGre model to account for the difference when the bodies transition from static friction to dynamic versus when the transition is from dynamic to static. They also made changes to the bristle state to make the dynamical model non-stiff at low relative velocities with a proper choice of model coefficients. Currently, this model shows promise as the results predicted by this model match well with experimental observations. For further review of friction model, the reader is referred to the paper by Marques on the topic [34]. Recent modeling approaches of hybrid dynamical systems may provide major breakthroughs in friction modeling, which is a just a specific case of a hybrid dynamical event. Taylor presents a MATLAB® based software package for hybrid dynamical systems and includes the example of stiction as a hybrid system [42].

The models discussed above fall in the category of *dynamic friction models* and are very versatile and capture the friction behavior really well. However, they are relatively difficult to implement due to their dependence on large number of parameters. Simpler models have been proposed each having their advantages and disadvantages. Some prominent ones are the smooth Coulomb model [43] which is a continuous and differentiable variant of the Coulomb friction model. However, it is incapable of modeling stiction. Karnopp model [44] is capable of modeling stiction to some extent and the sliding velocity within a certain *dead band* $|v| \leq v_d$ is as considered to be zero. Pennestrì et al. [45] have provided a comparative study of some of these models using a simulation of the Rabinowicz test [46].

A simple velocity-based friction model, primarily suited for control and real time applications was provided by Brown and McPhee [29]. This model is a continuous function of velocity and captures the Stribeck effect and viscous drag accurately. However, for the sake of simplicity, the micro-asperities and time dependence of friction have been omitted. This is expected, as inclusion of these phenomenon would lead to reduced performance of the model for real-time applications. The model has first order continuity and is differentiable which is important for sensitivity analysis. The authors also compare this model with other other friction models like Andersson model [47] and Specker et al. [48]. Brown and McPhee concluded that the Andersson model agrees with friction behavior with a smooth transition from rest velocity but the parameters used in the model are not very intuitive to understand and it is not entirely clear how they would affect the shape of the friction force-velocity curve. Moreover, both Specker and Andersson friction model predict viscous friction purely as a function of velocity and do not include the normal force in their formalism.

In conclusion of this review, it can be said that the Gonthier et al. friction model [31] and the Brown and McPhee friction model [29] are really well suited for multibody dynamic simulations. The detailed friction modeling and a comparative study of these two models has been presented in section 3.

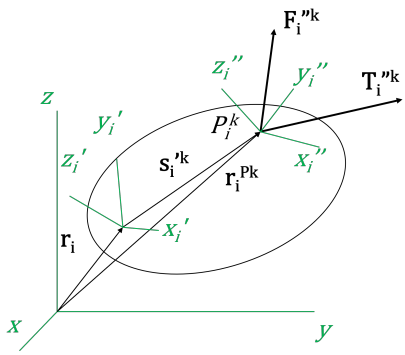

Fig. 1: Internal joint forces. Adapted from Haug [28].

3 Modeling

Models of spatial multibody systems are inherently non-linear due to the involvement of large rotations. Incorporation of joint friction to these models further adds to the complexity since the reaction forces at the joints are non-linear equations of the generalized coordinates and Lagrange multipliers. In the subsequent sections, the modeling of joint friction in multibody systems will be discussed. This process has been broken down into two independent tasks viz. the derivation of the normal force of contact at the joint interface and the computation of generalized friction force vector using the previously computed normal force and an appropriate friction model. It is implied in the following analysis that all terms involved in the equations of motion are functions of the system design parameters. This dependency has not been explicitly expressed.

3.1 Joint Normal Force of Contact

In any dynamical system there exist constraint forces and torques acting between two bodies at the joint interface. These constraint forces depend on the type of joint and the number of degrees of freedom the respective joint permits. Figure 1 shows these forces acting in the joint reference frame. Consider that the body i is connected to another body j (not shown in the figure) at point P_i^k. This means that there is a joint k at point P_i^k. Point P_i^k can be located on the body i through vector $\mathbf{s}_i'^k$ in the body-fixed reference frame $x'-y'-z'$. The body-fixed reference frame $x'-y'-z'$ can be located globally using the position vector $\mathbf{r}_i$. A joint reference frame $x''-y''-z''$ is defined at point P_i^k. The rotational transformation matrix from the reference frame $x''-y''-z''$ to the reference frame $x'-y'-z'$ is denoted by $\mathbf{C}_i^k$ and that between $x'-y'-z'$ and the global frame $x-y-z$ is given by $\mathbf{A}_i$. The constraint equations for the joint at point P_i^k are arranged in a vector $\mathbf{\Phi}^k$. Given this setup, Equation (1) gives the expression of these forces as derived by Haug [28].

$$\begin{bmatrix}\mathbf{F}_i''^k\\ \mathbf{T}_i''^k\end{bmatrix} = \begin{bmatrix}-\mathbf{C}_i^{k\mathrm{T}}\mathbf{A}_i^{\mathrm{T}}\mathbf{\Phi}_{\mathbf{r}_i}^{k\mathrm{T}}\boldsymbol{\lambda}^k\\ -\mathbf{C}_i^{k\mathrm{T}}\left(\frac{1}{2}\mathbf{G}(\mathbf{p}_i)\mathbf{\Phi}_{\mathbf{p}_i}^{k\mathrm{T}} - \tilde{\mathbf{s}}_i'^k\mathbf{A}_i^{\mathrm{T}}\mathbf{\Phi}_{r_i}^{k\mathrm{T}}\right)\boldsymbol{\lambda}^k\end{bmatrix} \tag{1}$$

These forces and torques are in arbitrary directions, as seen in Figure 2, and they need to be resolved along the joint

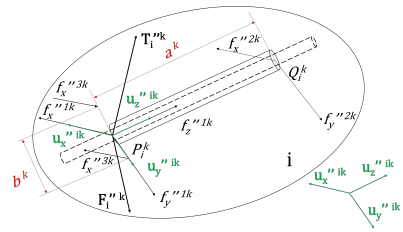

Fig. 2: Forces in a cylindrical joint. Adapted from Haug [28].

reference axes in order to compute the effective joint normal force F_n required to compute friction. Also, the reaction torque manifests itself as a couple acting along a moment arm, since moments applied at a point do not exist in real mechanisms. These forces acting as a couple constrain the bodies in rotational degrees of freedom and also contribute to the effective normal force F_n.

Haug [28] has provided the resolution of joint forces and torques for cylindrical, translational, and revolute joints. These joints can be modeled using a single joint type with different degrees of freedom as shown in Figure 2. Consequently, one model is sufficient to simulate the behavior for all three types of joints, the only difference being in their constraint forces. The main components of such a joint are the sleeve and the rod which guides it along a linear path. It is worth noting that the clearances in the joint required for smooth motion are assumed to be negligible relative to the magnitude of link displacements. Points P_i^k and Q_i^k represent the end contacts of the joint. The distance between these points is denoted by a^k. Similarly the width of the joint is denoted by b^k. These distances must be understood as a generic distance along which the constraint forces would act to restraint the degrees of freedom of the bodies, and must not be confused with the geometrical dimension of the joint. The torque $\mathbf{T_i}''^k$ and force $\mathbf{F_i}''^k$ from Equation (1) has been represented graphically in the figure. $\mathbf{u}_x''^{ik}$, $\mathbf{u}_y''^{ik}$ and $\mathbf{u}_z''^{ik}$ are unit vectors in the joint reference frame of body i. The main objective of this analysis is to get the components of the torque $\mathbf{T_i}''^k$ and force $\mathbf{F_i}''^k$ along the joint reference axes. The force components have been expressed in Equation (2).

$$f_x''^{1k} = -\mathbf{u}_x''^{ikT}\mathbf{F}_i''^k + \left(\frac{1}{a^k}\right)\mathbf{u}_y''^{ikT}\mathbf{T}_i''^k \tag{2a}$$

$$f_y''^{1k} = -\mathbf{u}_y''^{ikT}\mathbf{F}_i''^k - \left(\frac{1}{a^k}\right)\mathbf{u}_x''^{ikT}\mathbf{T}_i''^k \tag{2b}$$

$$f_x''^{2k} = -\left(\frac{1}{a^k}\right)\mathbf{u}_y''^{ikT}\mathbf{T}_i''^k \tag{2c}$$

$$f_y''^{2k} = \left(\frac{1}{a^k}\right)\mathbf{u}_x''^{ikT}\mathbf{T}_i''^k \tag{2d}$$

$$f_z''^{1k} = \mathbf{u}_z''^{ikT}\mathbf{F}_i''^k \tag{2e}$$

$$f_x''^{3k} = \left(\frac{1}{2b^k}\right)\mathbf{u}_z''^{ikT}\mathbf{T}_i''^k \tag{2f}$$

The components $f_z''^{1k}$ and $f_x''^{3k}$ will exist only for revolute and translational joints respectively. For computation of all the normal and friction forces, a continuous approximation to the absolute value function is required. This can be defined

as cabs(x) $= \sqrt{x^2+v_t^2}$. Now depending upon the type of joint, the effective normal force for the kth joint F_n^k can be calculated as follows:

1. For a cylindrical joint, the resultant normal force at both the joint end points will contribute to axial friction force. Considering a parabolic force distribution, the effective normal force is given by $F_n^k = f''^{1k} + f''^{2k}$ where $f''^{lk} = \frac{\pi^3}{24}\sqrt{(f_x''^{lk})^2 + (f_y''^{lk})^2 + v_t^2}$ and $l = 1, 2$. Additionally, there will be an induced friction torque at each end point given by whose magnitude is given by $\tau = r_e \operatorname{cabs}(F_f''^{lk})$, where r_e is the effective joint radius.
2. For a revolute joint, the treatment will be similar to a cylindrical joint with the addition of a thrust force in the z'' direction given by $\mathbf{u}_z''^{ikT}\mathbf{F}_i''^k$. This thrust force will contribute to a frictional torque about an effective torque radius r_e.
3. For a translational joint, the effective normal force is the absolute summation of all the force components. This is given by $F_n^k = \operatorname{cabs}(f_x''^{1k}) + \operatorname{cabs}(f_y''^{1k}) + \operatorname{cabs}(f_x''^{2k}) + \operatorname{cabs}(f_y''^{2k}) + 2\operatorname{cabs}(f_x''^{3k})$.

Now that the normal force acting at the joint interface has been computed, an appropriate friction model must be chosen for the dynamics. The subsequent sections present two different friction models, each having their advantages and drawbacks.

3.2 Joint friction force

Computation of generalized friction force for multibody systems is a two step process viz. computation of the magnitude of frictional force and torque at the joint and assembly of the generalized friction force vector. The former task will be detailed in the following subsections. For the generalized friction force vector, the friction force and torque vectors need to be computed about the center of mass of associated links. This is not a trivial task since the relative velocities in translation and rotation of links i and j (refer Figure 1) need to be computed to determine the direction of frictional forces and torques. Let the magnitude of the friction force along the axis of the cylindrical joint shown in Figure 2 be f_{ij} and the magnitude total frictional torque be τ_{ij}. For a revolute joint, $f_{ij} = 0$ and $\tau_{ij} = \tau_{ij}^{cyl.} + \tau_{ij}^{rev.}$, where $\tau_{ij}^{rev.}$ is the component due to axial thrust force. Similarly, for a translational joint $\tau_{ij} = 0$. The generalized friction for vector for body i can now be defined as shown in Equation (3).

$$\mathbf{Q}_i^{Af} = \begin{bmatrix} \mathbf{A}_i\mathbf{C}_i^k\mathbf{u}_z''^{ik} f_{ij} \\ \mathbf{B}_i^{\mathrm{T}}\mathbf{A}_i\mathbf{C}_i^k\mathbf{u}_z''^{ik} f_{ij} + 2\mathbf{E}_i^{\mathrm{T}}\mathbf{A}_i\mathbf{C}_i^k\mathbf{u}_z''^{ik}\tau_{ij} \end{bmatrix} \tag{3}$$

Naturally, by Newton's third law of motion, the generalized friction force vector for body j will be the additive inverse of the generalized friction force vector for body i i.e. $\mathbf{Q}_j^{Af} = -\mathbf{Q}_i^{Af}$. These individual generalized friction force vectors can be assembled to give the combined generalized friction force vector of the entire multibody system. Depending upon the assembly of the generalized coordinate vector $\mathbf{q}$, care must be taken to ensure the frictional forces are being added to applied forces and frictional torques to applied torques.

Two friction models have been used in this study for computation of the magnitude of friction force. The Brown and McPhee model is a static velocity-based model while the modified LuGre a.k.a. Gonthier et al. model is a dynamic model with two states. Brown McPhee model has been recommended by Haug for Lagrangian formulations [28]. The dynamical friction model developed by Gonthier et al. [31], was an improvement on the LuGre friction model [38]. It is a more realistic friction model that has shown significant accuracy when compared with the experimental behavior of friction and hence it will be used as a benchmark to evaluate the performance of the simpler Brown and McPhee model.

3.2.1 Joint Friction Model: Brown and McPhee

In 2016, Peter Brown and John McPhee at the University of Waterloo proposed a simple velocity based model designed primarily for optimal control and real-time dynamics. In this model, friction has been characterized as a continuous function of sliding velocity. To reduce model complexity, only the main velocity dependent characteristics of friction viz. the Stribeck effect, viscous friction were included, leaving out phenomena such as micro-displacement and the time dependence. The main advantage of this model to sensitivity analysis of multibody systems is its C^1 continuity and differentiability. What makes this friction model especially promising for dynamic systems is its ability to simulate stiction without any discontinuities in the stick-slip transition regime. Haug [28] applied the Brown and McPhee [29] model as an approximation to Coulomb friction acting at the joint interface between two bodies. Under the assumption that most mechanical systems are at least partially lubricated, the friction acting between such surfaces deviates from the dry Coulomb friction model. Coulomb friction being a discontinuous function of the sliding velocity during impending motion, or when the relative velocity is zero, Brown and McPhee friction model [29] characterized this region with a gradual increase in friction force magnitude. Most multibody systems may exhibit a viscous friction behavior, but for the sake of simplicity, the effect of viscous friction has been omitted in this work. Mathematically, such a friction model (without viscous friction) can be represented by Equation (4).

$$F_f(v,\boldsymbol{\mu}) = F_n\left[\mu_d \tanh\left(\frac{4v}{v_t}\right) + \frac{(\mu_s-\mu_d)\left(\frac{v}{v_t}\right)}{\left[\left(\frac{v}{2v_t}\right)^2 + \frac{3}{4}\right]^2}\right] \tag{4}$$

The transition velocity v_t is a difficult parameter to estimate in this model. Haug [28] recommends $v_t = 10h$ to $v_t = 20h$. Since v_t has the units of velocity and h that of time, it is worth noting that the coefficient of h is not a dimensionless number, so as to maintain unit consistency. Equation (4)

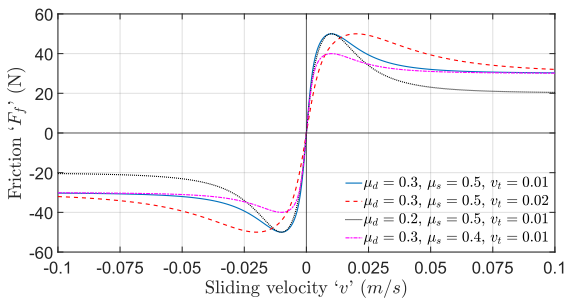

Fig. 3: Brown-McPhee friction model. $F_n = 100$ N.

has been visualized in Figure 3 for two different values of v_t, μ_d, and μ_s each and a normal force $F_n = 100$ N. From the graph it can be observed that, as the value of v_t reduces, the model tends to mimic the dry Coulomb friction model.

3.2.2 Joint Friction Model: Gonthier et al.

In 1995, a single state ODE formulation for friction was developed by de Wit et al. [38] as an extension of the Dahl model by combining stiction with Stribeck effects. The model has become popular in the research community as the *LuGre* model. Since it has been assumed in this model, that two rigid bodies interact with each other through elastic bristles, the friction force can be represented as a function of the bristle deformation $\mathbf{z}$ and the deformation rate $\dot{\mathbf{z}}$. The generated friction force from these bristles can be represented as $\mathbf{f}_{\text{br}} = \sigma_0\,\mathbf{z} + \sigma_1\,\dot{\mathbf{z}}$. Here σ_0 is the 'stiffness' of the bristles and σ_1 is a 'damping' coefficient for the bristle deformation rate. It is important to note that the ODEs given by this formulation are very stiff at low relative velocities, i.e. in the stiction regime, and need implicit ODE solvers. The time constant for the bristle dynamics is inversely proportional to the relative velocity, but the time constant for the overall system dynamics is small and constant during the stiction phase. Hence, a reformulation for the bristle state was done by Gonthier et al. [31]. The bristle state $\dot{\mathbf{z}}$ used in friction model Wit et al. was modified by Gonthier et al. into two distinct sub-models, viz. $\dot{\mathbf{z}}_{\text{st}}$ during the static friction regime and $\dot{\mathbf{z}}_{\text{sl}}$ for the sliding friction regime. A state variable s is responsible for the transitions from stick to slip phases and vice versa. Without going in the details of the derivation, the bristle deformation rate can be computed through the set of Equations (5)

$$\mathbf{f}_C = \mu_d\,F_n\,\text{dir}_\varepsilon\left(\mathbf{u}_{ij},\,v_\varepsilon\right) \tag{5a}$$

$$\text{dir}_\varepsilon\left(\mathbf{u}_{ij},\,v_\varepsilon\right) = \begin{cases} \frac{\mathbf{u}_{ij}}{|\mathbf{u}_{ij}|}; & |\mathbf{u}_{ij}| \geq v_\varepsilon \\ \frac{\mathbf{u}_{ij}}{v_\varepsilon}\left(\frac{3}{2}\cdot\frac{|\mathbf{u}_{ij}|}{v_\varepsilon} - \frac{1}{2}\left(\frac{|\mathbf{u}_{ij}|}{v_\varepsilon}\right)^3\right); & |\mathbf{u}_{ij}| < v_\varepsilon \end{cases} \tag{5b}$$

$$\dot{\mathbf{z}} = s\,\mathbf{u}_{ij} + (1-s)\left(\frac{1}{\sigma_1}\mathbf{f}_C - \frac{\sigma_0}{\sigma_1}\mathbf{z}\right) \tag{5c}$$

Additionally, Gonthier et al. also incorporated the dwell-time dependency during the static friction phase to accurately model the transition from static friction to sliding. The way it is incorporated in the model is by introducing a new state s_{dw}. The dynamics for this state are defined as follows

$$\dot{s}_{\text{dw}} = \begin{cases} \frac{1}{\tau_{\text{dw}}}\left(s - s_{\text{dw}}\right); & s - s_{\text{dw}} \geq 0 \\ \frac{1}{\tau_{\text{br}}}\left(s - s_{\text{dw}}\right); & s - s_{\text{dw}} < 0 \end{cases} \tag{6}$$

Here τ_{dw} is the dwell-time dynamics time constant, and it is one of the parameters of the model. The overall friction force can now be computed through the set of Equations 7

$$f_{max} = F_n\left(\mu_d + (\mu_s - \mu_d)\,s_{\text{dw}}\right) \tag{7a}$$

$$\text{sat}\left(\mathbf{f}_{\text{br}},\,f_{\text{max}}\right) = \begin{cases} \mathbf{f}_{\text{br}}; & |\mathbf{f}_{\text{br}} \leq f_{\text{max}}|, \\ \frac{\mathbf{f}_{\text{br}}}{|\mathbf{f}_{\text{br}}|}\,f_{\text{max}}; & |\mathbf{f}_{\text{br}} > f_{\text{max}}| \end{cases} \tag{7b}$$

$$\mathbf{F}_f = -\left(\text{sat}\left(\mathbf{f}_{\text{br}},\,f_{\text{max}}\right) + \sigma_2\,\mathbf{u}_{ij}\right) \tag{7c}$$

As it can be observed, that the friction model proposed by Gonthier et al. involves seven independent parameters; μ_s, μ_d, σ_0, σ_1, σ_2, v_s, and τ_{dw}. Unlike the Brown and McPhee model, friction is directly computed in the form of a vector using the Gonthier et al. model.

3.2.3 Rabinowicz Stiction Experiment

In the previous sections, two different friction models were discussed. In order to compare these models, with their relative advantages and drawbacks, a simple test case is presented in the following sections. An experiment was proposed in 1938 by Bowden and Leben to study the *stick-and-slip* nature of friction. In 1961, Rabinowicz [46] gave a more formal treatment to this experiment. This experiment can be modeled numerically to test out different friction models, as it can be seen in literature [34,45]. A simulation was created in MATLAB® for benchmarking Brown and McPhee friction model against Gonthier friction model. The simulation parameters have been listed in Table 1

Table 1: Bowden-Leben experiment parameters.

Par.	**Val.**	**Par.**	**Val.**
m	1 kg	g	10 m/s^2
k	2 N/m	v	0.15 m/s
μ_s	0.4	μ_d	0.3
σ_0	10^5 N/m	σ_1	$\sqrt{10^5}$ N-s/m
σ_2	0 N-s/m	τ_{dw}	2 s
v_ε	1.5e-7 m/s	$v_s = v_t$	1.5e-3 m/s

The experiment was simulated for a total of 40 seconds. Figure 4 plots the friction force computed by Brown and McPhee model versus that computed by Gonthier et al. model. As it can be observed, the force magnitudes given by both models are very similar with minor differences, especially during the transition phases i.e. from stiction to sliding friction. This is expected since the characterization of this

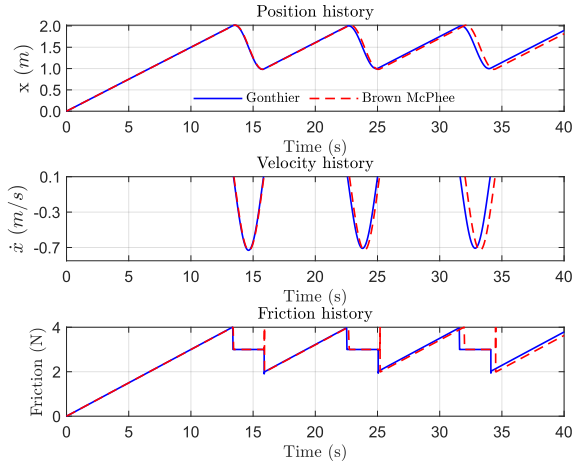

Fig. 4: Absolute position and velocity of the block.

regime is much more accurate in the Gonthier et al. model. However, since this transition happens over a very brief time, the loss of accuracy in Brown and McPhee model is insignificant. Likewise, the position and velocity plots are also very similar in both models.

As per the numerical simulation of the Bowden Leben experiment, the Brown and McPhee model is found to be capable of simulating reasonably accurate friction behavior despite its modeling simplicity. Hence, it proves to be a good starting point for performing sensitivity analysis of multibody systems with friction.

4 Forward Dynamics

The time history of multibody systems forms the basis for sensitivity analysis and dynamical optimization. The index-1 constrained equations of motion for scleronomic multibody systems in centroidal generalized coordinates with joint friction can be written as

$$\mathbf{R} = \mathbf{M}(\mathbf{q})\ddot{\mathbf{q}} + \mathbf{\Phi}_{\mathbf{q}}^{\mathrm{T}}(\mathbf{q})\boldsymbol{\lambda} - \mathbf{Q}^{Af}(\mathbf{q},\dot{\mathbf{q}},\boldsymbol{\lambda}) - \mathbf{Q}(\mathbf{q},\dot{\mathbf{q}}) = \mathbf{0} \quad (8a)$$

$$\mathbf{\Phi}_{\mathbf{q}}\ddot{\mathbf{q}} + (\mathbf{\Phi}_{\mathbf{q}} \cdot \dot{\mathbf{q}})_{\mathbf{q}} \cdot \dot{\mathbf{q}} = \mathbf{0} \quad (8b)$$

Equation (8) can be written in a matrix notation as follows

$$\begin{bmatrix} \mathbf{M} & \mathbf{\Phi}_{\mathbf{q}}^{\mathrm{T}} \\ \mathbf{\Phi}_{\mathbf{q}} & \mathbf{0} \end{bmatrix} \begin{bmatrix} \ddot{\mathbf{q}} \\ \boldsymbol{\lambda} \end{bmatrix} = \begin{bmatrix} \mathbf{Q} + \mathbf{Q}^{Af} \\ \mathbf{c} \end{bmatrix} \quad (9)$$

Equation (9) needs to satisfy the constraint equations for initial positions $\mathbf{q}_0$ and velocities $\dot{\mathbf{q}}_0$ at the initial time t_0. These are given by Equation (10)

$$\mathbf{\Phi}\big|_{t_0} = \mathbf{0} \implies \mathbf{\Phi}_{\mathbf{q}}\big|_{t_0} \Delta\mathbf{q}^i = -\mathbf{\Phi}\big|_{t_0} \quad (10a)$$

$$\mathbf{q}^{i+1} = \mathbf{q}^i + \Delta\mathbf{q}^i \quad (10b)$$

$$\dot{\mathbf{\Phi}}\big|_{t_0} = \mathbf{0} \implies \mathbf{\Phi}_{\mathbf{q}}\big|_{t_0} \dot{\mathbf{q}} = \mathbf{0} \quad (10c)$$

It is important to note that Equation (10a) cannot be solved by matrix inversion as $\mathbf{\Phi}_{\mathbf{q}}$ is typically a rectangular matrix $(m \times n)$. One approach for solving this equation, is to simply add $n-m$ temporary constraints to the $\mathbf{\Phi}$ vector which specify the initial positions of the $(n-m)$ independent generalized coordinates. This makes the Jacobian $\mathbf{\Phi}_{\mathbf{q}}$ an $n \times n$ square matrix which can be inverted to compute the initial positions. The solution would require an initial estimate of the generalized coordinates $\mathbf{q}$ since the constraints $\mathbf{\Phi}$ and Jacobian $\mathbf{\Phi}_{\mathbf{q}}$ both depend on $\mathbf{q}$. This estimate can be converged to a high accuracy using Newton's iteration as shown in Equations (10a) and (10b). For spatial systems, obtaining a reasonably good estimate of $\mathbf{q}$ is a challenge and typically requires a CAD model. Poor estimates of generalized coordinates are prone to divergence which lead to singular constraint Jacobian matrix. The solution for the initial velocity vector $\dot{\mathbf{q}}$ is a bit more involved. The trivial solution $\dot{\mathbf{q}} = \mathbf{0}$ will always satisfy Equation (10c) but for non-zero initial velocities, the solution has to be a linear combination of the null space vectors of $\mathbf{\Phi}_{\mathbf{q}}$ at the initial time such that the velocities of the $(n-m)$ independent coordinates are satisfied. It is implied in this analysis that the constraint Jacobian is full rank.

It can be noted that in Equation (9), the Lagrange multipliers $\boldsymbol{\lambda}$ are present on both sides of the Equation, since $\mathbf{Q}^{Af}$ depends on the joint normal force which in turn depends on the Lagrange multipliers. Equation (9) would have been linear in the Lagrange multipliers if joint friction was absent from the model. However, if joint friction force exists in the system at the very first time step (for example, if the mechanism is already in motion), then Lagrange multipliers $\boldsymbol{\lambda}$ and accelerations $\ddot{\mathbf{q}}$ need to be converged simultaneously. Unlike the generalized coordinates, it is very difficult to obtain estimates for Lagrange multipliers at the first time step. Hence a fixed-point iteration needs to be implemented on Equation (9) by assuming an initial value of the Lagrange multipliers till $|\mathbf{R}| \leq \delta$. In this analysis the initial estimate of Lagrange multipliers can be chosen from a random normal distribution or taken as a zero vector.

The other numerical aspect that needs to be considered is the stiffness of the index-1 formulation due to the presence of second derivatives of the constraint equations. Explicit integration schemes do not work well with these formulations. The implicit trapezoidal integration scheme is better suited to handle the stiffness associated with the index-1 equations of motion. The second order implicit trapezoidal scheme has been expressed in Equation (11).

$$\mathbf{v}^{i+1} = \mathbf{v}^i + h\dot{\mathbf{v}}^i + \frac{h^2}{4}(\ddot{\mathbf{v}}^i + \ddot{\mathbf{v}}^{i+1}) \quad (11a)$$

$$\dot{\mathbf{v}}^{i+1} = \dot{\mathbf{v}}^i + \frac{h}{2}(\ddot{\mathbf{v}}^i + \ddot{\mathbf{v}}^{i+1}) \quad (11b)$$

The implementation of this scheme to compute the time

history for a multibody system modeled using index-1 formulation is given in Algorithm 1.

for $t < t_f$ **do**
  $\left[\ddot{\mathbf{q}}; \boldsymbol{\lambda}\right] = \mathbf{f}(\mathbf{q}, \dot{\mathbf{q}}, \boldsymbol{\lambda})$ (say);
  save $\mathbf{q}, \dot{\mathbf{q}}, \ddot{\mathbf{q}}$ and $\boldsymbol{\lambda}$ against current time t;
  $\mathbf{q}_{pred} = \mathbf{q} + h\dot{\mathbf{q}} + 0.25h^2\ddot{\mathbf{q}}$;
  $\dot{\mathbf{q}}_{pred} = \dot{\mathbf{q}} + 0.5h\ddot{\mathbf{q}}$;
  $i = 0$, $\varepsilon = 1.0$, $\delta = 10^{-4}$, $\aleph = 10^3$;
  while $\varepsilon < \delta$ ***and*** $i < \aleph$ **do**
    $\mathbf{q} = \mathbf{q}_{pred} + 0.25h^2\ddot{\mathbf{q}}$;
    $\dot{\mathbf{q}} = \dot{\mathbf{q}}_{pred} + 0.5h\ddot{\mathbf{q}}$;
    $\ddot{\mathbf{q}}^* = \ddot{\mathbf{q}}$;
    $\left[\ddot{\mathbf{q}}; \boldsymbol{\lambda}\right] = \mathbf{f}(t, \mathbf{q}, \dot{\mathbf{q}}, \boldsymbol{\lambda})$;
    $\varepsilon = 0.25h^2\|\ddot{\mathbf{q}} - \ddot{\mathbf{q}}^*\|$;
    $i = i + 1$;
  end
end

Algorithm 1: Implicit trapezoidal integration.

It must be noted however, that the satisfaction of acceleration constraints $\ddot{\boldsymbol{\Phi}}$ to a numerical precision $\boldsymbol{\varepsilon}$ or the use of implicit integration schemes is not sufficient to automatically satisfy the position $\boldsymbol{\Phi}$ or the velocity constraints $\dot{\boldsymbol{\Phi}}$. For position constraints, this error propogates quadratically in time since $\boldsymbol{\Phi} = \boldsymbol{\varepsilon}t^2 + \mathbf{c}_1 t + \mathbf{c}_2$ where $\mathbf{c}_1$ and $\mathbf{c}_2$ are constants of integration. However, this effect is much more noticeable in explicit integration schemes than the implicit trapezoidal scheme. To more effectively handle this constraint drift, the time step h should be kept small. It has been taken as 10^{-4} seconds in this analysis. For long simulations, it is recommended to reconcile the constraints periodically to keep the drift bounded. There has been development of formulations for multibody systems which are much more well-behaved [49], however the use Lagrangian formulations is better suited for dynamics and sensitivity analysis of systems involving friction.

5 Sensitivity Analysis

The direct differentiation method can be applied to the index-1 formulation that was discussed in the previous section. Dopico et al. [50] consider the objective function of the form

$$\boldsymbol{\psi} = \mathbf{w}\left(\mathbf{q}_f, \dot{\mathbf{q}}_f, \ddot{\mathbf{q}}_f, \boldsymbol{\lambda}_f, \boldsymbol{\rho}_f\right) + \int_{t_o}^{t_f} \mathbf{g}(\mathbf{q}, \dot{\mathbf{q}}, \ddot{\mathbf{q}}, \boldsymbol{\lambda}, \boldsymbol{\rho})\,\mathrm{d}t \quad (12)$$

Here $\boldsymbol{\psi} \in \mathbb{R}^o$, is a vector of '$o$' objective functions, whereas $\mathbf{w} \in \mathbb{R}^o$ and $\mathbf{g} \in \mathbb{R}^o$ are the pointwise term at the final time (hence the subscript 'f') and the integrand for each one of the objective functions respectively. The gradient of the objective function is given by

$$\begin{aligned}\nabla_{\boldsymbol{\rho}}\boldsymbol{\psi}^{\mathrm{T}} = &\left(\mathbf{w}_{\mathbf{q}}\mathbf{q}_{\boldsymbol{\rho}} + \mathbf{w}_{\dot{\mathbf{q}}}\dot{\mathbf{q}}_{\boldsymbol{\rho}} + \mathbf{w}_{\ddot{\mathbf{q}}}\ddot{\mathbf{q}}_{\boldsymbol{\rho}} + \mathbf{w}_{\boldsymbol{\lambda}}\boldsymbol{\lambda}_{\boldsymbol{\rho}} + \mathbf{w}_{\boldsymbol{\rho}}\right)_f \\ &+ \int_{t_o}^{t_f}\left(\mathbf{g}_{\mathbf{q}}\mathbf{q}_{\boldsymbol{\rho}} + \mathbf{g}_{\dot{\mathbf{q}}}\dot{\mathbf{q}}_{\boldsymbol{\rho}} + \mathbf{g}_{\ddot{\mathbf{q}}}\ddot{\mathbf{q}}_{\boldsymbol{\rho}} + \mathbf{g}_{\boldsymbol{\lambda}}\boldsymbol{\lambda}_{\boldsymbol{\rho}} + \mathbf{g}_{\boldsymbol{\rho}}\right)\mathrm{d}t\end{aligned} \quad (13)$$

In this equation, since $\mathbf{w}$ and $\mathbf{g}$ are chosen as per the optimization objective, the derivatives of functions $\mathbf{w}$ and $\mathbf{g}$ can be computed. It is important to note that in Equation (13), the terms $\mathbf{q}_{\boldsymbol{\rho}}$, $\dot{\mathbf{q}}_{\boldsymbol{\rho}}$, $\ddot{\mathbf{q}}_{\boldsymbol{\rho}}$ and $\boldsymbol{\lambda}_{\boldsymbol{\rho}}$ are total derivatives with respect to the parameters, unlike the other terms which are partial derivatives. These are the sensitivities of the dynamical system with respect to the system parameters. To calculate these sensitivities, Equation (8) is differentiated with respect to each one of the parameters. This step has been represented in Equation (14).

$$\frac{\mathrm{d}\mathbf{R}}{\mathrm{d}\rho_k} = \frac{\mathrm{d}\mathbf{M}(\mathbf{q})\ddot{\mathbf{q}}}{\mathrm{d}\rho_k} + \frac{\mathrm{d}\boldsymbol{\Phi}_{\mathbf{q}}^{\mathrm{T}}(\mathbf{q})\boldsymbol{\lambda}}{\mathrm{d}\rho_k} - \frac{\mathrm{d}(\mathbf{Q}^{Af}(\mathbf{q}, \dot{\mathbf{q}}, \boldsymbol{\lambda}) + \mathbf{Q}(\mathbf{q}, \dot{\mathbf{q}}, t))}{\mathrm{d}\rho_k} \quad (14a)$$

$$\frac{\mathrm{d}\ddot{\boldsymbol{\Phi}}}{\mathrm{d}\rho_k} = \mathbf{0}, \quad k = 1, 2, ..., p \quad (14b)$$

Assuming all of the terms depend on $\boldsymbol{\rho}$, the total derivatives can be expanded and rearranged to give a set of 'p' Tangent Linear Models (TLMs).

$$\begin{aligned}&\mathbf{M}\ddot{\mathbf{q}}_{\rho_k} + (\mathbf{C} + \mathbf{C}^{Af})\dot{\mathbf{q}}_{\rho_k} + (\boldsymbol{\Phi}_{\mathbf{q}}{}^{\mathrm{T}} + \mathbf{L}^{Af})\boldsymbol{\lambda}_{\rho_k} \\ &\quad + \left[\mathbf{M}_{\mathbf{q}}\ddot{\mathbf{q}} + \boldsymbol{\Phi}_{\mathbf{qq}}{}^{\mathrm{T}}\boldsymbol{\lambda} + (\mathbf{K} + \mathbf{K}^{Af})\right]\mathbf{q}_{\rho_k} \\ &\quad = \mathbf{Q}_{\rho_k} + \mathbf{Q}_{\rho_k}{}^{Af} - \mathbf{M}_{\rho_k}\ddot{\mathbf{q}} - \boldsymbol{\Phi}_{\mathbf{q}\rho_k}{}^{\mathrm{T}}\boldsymbol{\lambda}\end{aligned} \quad (15a)$$

$$\boldsymbol{\Phi}_{\mathbf{q}}\ddot{\mathbf{q}}_{\rho_k} - \mathbf{c}_{\dot{\mathbf{q}}}\dot{\mathbf{q}}_{\rho_k} + (\boldsymbol{\Phi}_{\mathbf{qq}}\ddot{\mathbf{q}} - \mathbf{c}_{\mathbf{q}})\mathbf{q}_{\rho_k} = \mathbf{c}_{\rho_k} - \boldsymbol{\Phi}_{\mathbf{q}\rho_k}\ddot{\mathbf{q}} \quad (15b)$$

where $\mathbf{K} = -\mathbf{Q}_{\mathbf{q}}$, $\mathbf{C} = -\mathbf{Q}_{\dot{\mathbf{q}}}$, $\mathbf{K}^{Af} = -\mathbf{Q}_{\mathbf{q}}{}^{Af}$, $\mathbf{C}^{Af} = -\mathbf{Q}_{\dot{\mathbf{q}}}{}^{Af}$, $\mathbf{L}^{Af} = -\mathbf{Q}_{\lambda}{}^{Af}$, $\mathbf{c}_{\mathbf{q}} = -\dot{\boldsymbol{\Phi}}_{\mathbf{qq}}\dot{\mathbf{q}}$, $\mathbf{c}_{\dot{\mathbf{q}}} = -\dot{\boldsymbol{\Phi}}_{\mathbf{q}\dot{\mathbf{q}}}\dot{\mathbf{q}} - \dot{\boldsymbol{\Phi}}_{\mathbf{q}}$, and $\mathbf{c}_{\rho_k} = -\dot{\boldsymbol{\Phi}}_{\mathbf{q}\rho_k}\dot{\mathbf{q}}$.

In Equation (15), frictional force vector $\mathbf{Q}^{Af}$, and the corresponding stiffness and damping matrices $\mathbf{K}^{Af}$, $\mathbf{C}^{Af}$ and $\mathbf{L}^{Af}$ are all dependent on Lagrange multipliers. In this work reference point coordinates have been used with Euler parameters for rotation ($n = 7nb$). It has been assumed that $\boldsymbol{\Phi}$ does not contain any time-dependent constraints. It is noteworthy that the terms $\mathbf{M}_{\mathbf{q}}\ddot{\mathbf{q}}$ and $\boldsymbol{\Phi}_{\mathbf{qq}}^{\mathrm{T}}\boldsymbol{\lambda}$ are tensor-vector products. Essentially, $\mathbf{M}_{\mathbf{q}}$ and $\boldsymbol{\Phi}_{\mathbf{qq}}$ are three-dimensional matrices where the nth *layer* along the *depth* is a two-dimensional matrix formed by the partial derivatives of the original matrix elements with respect to the nth element in the differentiating vector. During the tensor-vector product, each of these *layers* multiplies with a vector as a matrix-vector multiplication, and the resultant vectors can be arranged sequentially to form a two-dimensional matrix.

For the solution of Equation (15), a set of $2np$ initial conditions as given by $\mathbf{q}_{\rho_k}\big|_{t_0} = \mathbf{q}_{\rho_k 0}$ and $\dot{\mathbf{q}}_{\rho_k}\big|_{t_0} = \dot{\mathbf{q}}_{\rho_k 0}$. Since

the initial conditions have to satisfy the constraints at the initial time, they can be computed by solving Equation (16).

$$\left.\frac{\mathrm{d}\boldsymbol{\Phi}}{\mathrm{d}\rho_k}\right|_{t_0} = \mathbf{0} \implies \boldsymbol{\Phi}_{\mathbf{q}}\big|_{t_0}\,\mathbf{q}_{\rho_k 0} = -\boldsymbol{\Phi}_{\rho_k}\big|_{t_0} \tag{16a}$$

$$\left.\frac{\mathrm{d}\dot{\boldsymbol{\Phi}}}{\mathrm{d}\rho_k}\right|_{t_0} = \mathbf{0} \implies \boldsymbol{\Phi}_{\mathbf{q}}\big|_{t_0}\,\dot{\mathbf{q}}_{\rho_k 0} = -\left(\boldsymbol{\Phi}_{\mathbf{qq}}\mathbf{q}_{\rho_k 0} + \boldsymbol{\Phi}_{\mathbf{q}\rho_k}\right)\dot{\mathbf{q}}\big|_{t_0} \tag{16b}$$

Rearranging Equation (15) in an augmented matrix form as shown in Equation (17), it can be solved for $\ddot{\mathbf{q}}_{\rho_k}$ and $\boldsymbol{\lambda}_{\rho_k}$ by simple matrix inversion.

$$\begin{bmatrix} \mathbf{M} & \boldsymbol{\Phi}_{\mathbf{q}}^{\mathrm{T}} + \mathbf{L}^{Af} \\ \boldsymbol{\Phi}_{\mathbf{q}} & \mathbf{0} \end{bmatrix} \begin{bmatrix} \ddot{\mathbf{q}}_{\rho_k} \\ \boldsymbol{\lambda}_{\rho_k} \end{bmatrix} = \begin{bmatrix} \mathbf{A} \\ \mathbf{B} \end{bmatrix} \tag{17}$$

where $\mathbf{A} = \mathbf{Q}_{\rho_k} + \mathbf{Q}_{\rho_k}{}^{Af} - \mathbf{M}_{\rho_k}\ddot{\mathbf{q}} - \boldsymbol{\Phi}_{\mathbf{q}\rho_k}{}^{\mathrm{T}}\boldsymbol{\lambda} - (\mathbf{C} + \mathbf{C}^{Af})\dot{\mathbf{q}}_{\rho_k} - \left[\mathbf{M}_{\mathbf{q}}\ddot{\mathbf{q}} + \boldsymbol{\Phi}_{\mathbf{qq}}{}^{\mathrm{T}}\boldsymbol{\lambda} + (\mathbf{K} + \mathbf{K}^{Af})\right]\mathbf{q}_{\rho_k}$ and $\mathbf{B} = \mathbf{c}_{\rho_k} - \boldsymbol{\Phi}_{\mathbf{q}\rho_k}\ddot{\mathbf{q}} + \mathbf{c}_{\dot{\mathbf{q}}}\dot{\mathbf{q}}_{\rho_k} - (\boldsymbol{\Phi}_{\mathbf{qq}}\ddot{\mathbf{q}} - \mathbf{c}_{\mathbf{q}})\mathbf{q}_{\rho_k}$

It must be noted that the sensitivities of marginally stable systems might not be marginally stable since the system dynamics feed into the tangent linear model of the sensitivities, effectively acting as a destabilizing input [12]. This is not a concern for systems with friction/damping, since they are open-loop stable.

6 Validation of analytical sensitivities

In section 5, the analytical methodology to calculate sensitivities was developed. However, it is possible to numerically compute these sensitivities using the Finite Difference Method (FDM) without the need to mathematically differentiate the equations of motion. In this technique the model parameters with respect to which the sensitivities have to be computed are modified with a very small but numerically significant perturbation in order to obtain the corresponding effect in the output of the model. This perturbation can be real or imaginary in nature which leads to two different strategies to obtain the sensitivities. If the perturbation is real, the sensitivities can be approximated by using Equation (18).

$$\frac{\mathrm{d}\psi}{\mathrm{d}\rho_k} = \frac{\psi(\boldsymbol{\rho} + \delta\mathbf{e}_k) - \psi(\boldsymbol{\rho})}{\delta} \tag{18}$$

Although this approach is relatively simple, using real finite differences is not recommended as the results may not be accurate. Since the method involves very small differences, it is prone to loss-of-significance error due to numerical truncation. To avoid these issues a complex finite difference method can be employed. In this method the perturbations in the model parameters are imaginary leading to complex model outputs. The sensitivities can be computed by using Equation (19).

$$\frac{\mathrm{d}\psi}{\mathrm{d}\rho_k} = \frac{\Im(\psi(\boldsymbol{\rho} + i\delta\mathbf{e}_k))}{\delta} \tag{19}$$

where $i = \sqrt{-1}$ and $\Im(\cdot)$ represents the imaginary part of a complex number. Complex finite difference method is much more reliable and accurate than its real counterpart due to the absence of subtraction. However the software package being used and the dynamic model should be able to accommodate complex numbers especially while using traditionally real functions such as trigonometric functions, integration schemes, norm, absolute value, sign functions etc. to name a few.

7 Case Study : Spatial Slider Crank Mechanism

The theory that was developed in the previous sections has been applied to obtain the design sensitivities of a spatial slider crank mechanism. The objective of this study is to analyze the effect of friction on the dynamics and model sensitivities. Additionally, numerical aspects associated with integration of forward dynamics, and computation of Lagrange multipliers will be demonstrated. Also, the sensitivities obtained with the analytical method have been compared to those obtained through complex FDM for comparison.

The model has been adapted from Haug (1989) [51] where the kinematic analysis of the mechanism has been presented. However, for the purpose of dynamic analysis, the body-fixed reference frame on the crank has been relocated to its center of gravity. Also, the joint between the connecting rod and slider has been modeled as a single universal joint, unlike the two separate constraints used in Haug (1989) [51]. Two models of this mechanism were created in MATLAB® using the Symbolic Math Toolbox™. The first model is frictionless (Model 1), while the other (Model 2) has been implemented with friction at the slider-ground interface. Once all the symbolic matrices required for dynamics and sensitivity calculation have been determined, the models are converted into numerical functions for faster solution times. The dynamics and sensitivities have been computed for both models moving under the action of gravity. The model schematic can be seen in Figure 5. The dimensions represent the configuration of the model at the moment of its initialization in the numerical simulation.

7.1 Dynamics and Numerical Aspects

The model mass and inertia properties have been summarized in Table 2. For friction parameters, please refer to Table 1. As mentioned previously, initialization of the model from non-zero generalized velocity requires the convergence of Lagrange multipliers for the first time step using a fixed-point iteration. Figure 6 demonstrates the convergence of the Lagrange multipliers and the acceleration at the very first time step for a slider velocity of 1 m/s. The

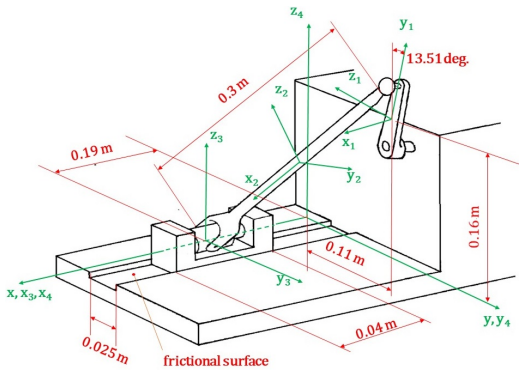

Fig. 5: Slider-crank mechanism schematic.

Table 2: Simulation parameters

Link	**Mass (kg)**	**Inertia (g-m^2)**
Crank	0.0771	$[0.1644, 0.01644, 0.164]^{\mathrm{T}}$
Connecting Rod	1.3317	$[0.9988, 9.988, 9.988]^{\mathrm{T}}$
Slider	0.2	$[1.5, 1.5, 1.5]^{\mathrm{T}}$
Ground	20	$[10^3, 10^3, 10^3]^{\mathrm{T}}$

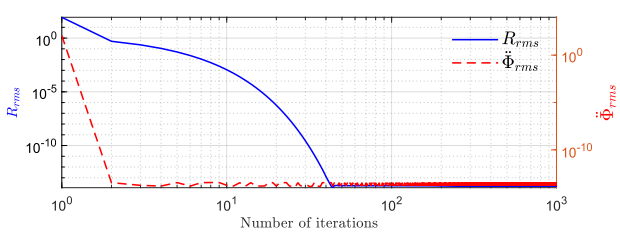

Fig. 6: Fixed-point iteration of dynamics.

existence of a fixed-point and the convergence of this iteration has been assumed to work for physical second-order systems, of which multibody dynamic systems are a subset. The mathematical treatment of the criteria for existence of solution is beyond the scope for this work.

To demonstrate the error control due to the stiffness of the index-1 formulation, Model 1 was simulated using both forward Euler and implicit trapezoidal integration schemes. Effectively such a system should give an oscillatory response lasting indefinitely as there are no energy leaks from the system. However, due to constraint violation the dynamic response deviates from this behavior. Figure 7 shows the violation in acceleration, velocity and position constraints using both the integration schemes. As it can be inferred from the plots, the error stays bounded if an implicit trapezoidal integration scheme is used.

Now that the numerical aspects associated with the index-1 formulation with friction have been resolved, the dynamics of the spatial slidercrank mechanism can now be computed. Since this case study will be used to validate the proposed sensitivity methodology, unnecessary inputs to the model that may complicate the dynamics and sensitivity plots have been avoided. The model is initiated in an unstable configuration as shown in Figure 5, such that it moves

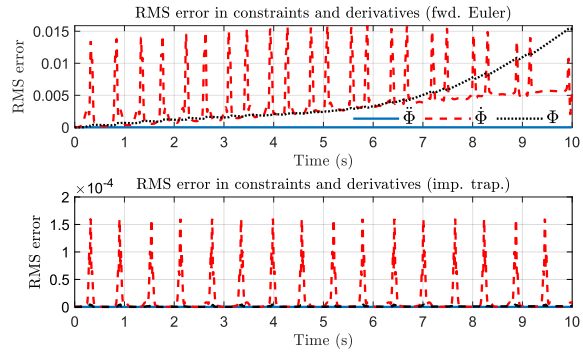

Fig. 7: Constraint error control using Implicit integration.

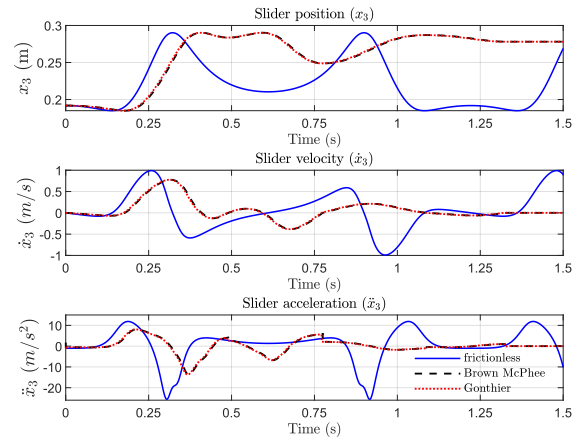

Fig. 8: Time history of slider C.G.

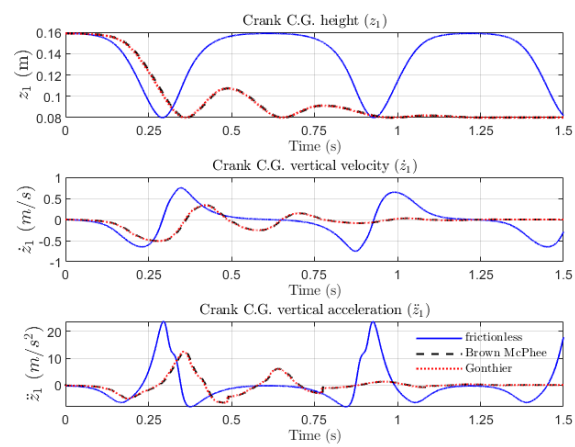

Fig. 9: Time history of crank C.G.

solely under the action of gravity. Since, no external energy is being added into the system, the response of the mechanism should be similar to a periodic oscillation with Model 2 exhibiting energy dissipation through frictional damping. Figure 8 shows the position, velocity and acceleration plots of the slider. The dynamic response of the system is very similar for both friction models. The energy dissipation due to friction is evident in Figure 9, which plots the height of the center of gravity of the crank.

Figure 10 shows the variation of normal force and con-

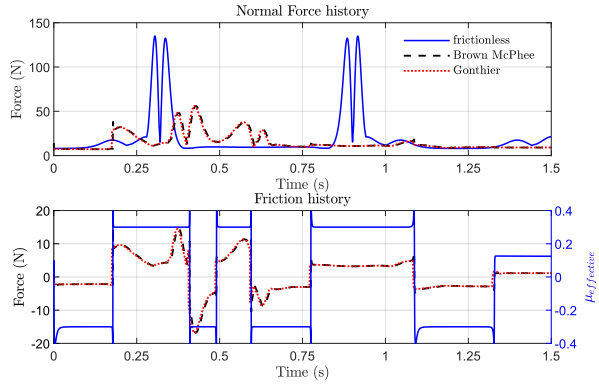

Fig. 10: Friction time history.

sequently the friction force over time. The coupling between the normal force and friction force due to the inclination of the connecting rod is clearly evident. The effective normal force will always be 'positive', since friction acts irrespective of the direction of the normal force. The normal force is much higher for frictionless model when the mechanism is at peak velocity, however at all other times, the normal force is higher for the model with joint friction. This is due to a portion of the frictional force being taken up by the rod due to its orientation in space and transferred back to the slider as a normal force.

7.2 Sensitivity Analysis

For sensitivity analysis of the spatial slider-crank mechanism, a few physically meaningful parameters must be chosen. Additionally, these parameters must be such that they can be engineered to meet a certain performance criteria. Naturally, the choice of these parameters depends on the objective function $\boldsymbol{\psi}$ chosen in Equation (12). For this analysis, the sensitivities have been computed with respect to crank length ($\rho_1 = 0.08$ m), connecting rod length ($\rho_2 = 0.3$ m), the width and length of the slider ($\rho_3 = 0.025$ m and $\rho_4 = 0.05$ m) and the friction parameters $\mu_d = 0.4$, $\mu_s = 0.5$ and $v_t = 1.5 \times 10^{-3}$ (ρ_5, ρ_6 and ρ_7). For the frictionless model, only sensitivities with respect to crank and connecting rod length can be observed as it does not have any dependency on the other parameters. It must be noted that the masses and inertia of linkages will depend on some of these parameters and hence the mass matrix '**M**' will be a function of these parameters. For this study however, the masses and inertia of the links have been assumed to be independent of these parameters.

Regarding model sensitivities, it is noteworthy that these time-dependent quantities are difficult to interpret on their own. The magnitudes of sensitivities give some insight into which parameters have the most impact on the model dynamics of interest. However, the most practical use of the computed sensitivities is in the evaluation of the gradient function $\nabla_{\boldsymbol{\rho}} \boldsymbol{\psi}$ in Equation (13).

$$\bar{\mathbf{S}} = \rho \frac{\mathrm{d}x}{\mathrm{d}\rho} \approx \frac{\Delta x}{\frac{\Delta \rho}{\rho}} \tag{20}$$

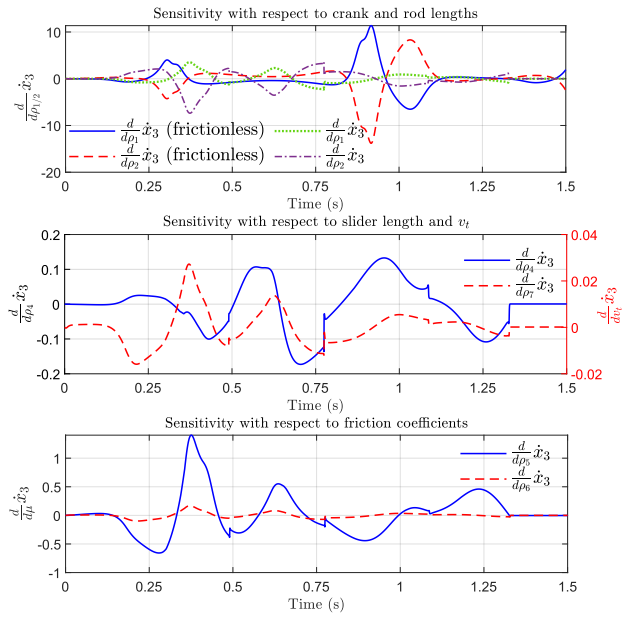

Fig. 11: Scaled sensitivities.

In this study, the dynamic quantity that has been considered for the purpose of sensitivity analysis is the slider velocity as it is a critical design parameter for many applications. Equations (20) describe a scaling technique that has been used to help compare sensitivities of different parameters irrespective of their units or magnitude. These scaled sensitivities for all the parameters have been plotted in Figure 11.

There are few things to be noted from the sensitivity plots. Firstly the sensitivities of the slider velocity are highest with respect to the crank and connecting rod lengths. In other words, slider velocity is affected much more significantly by changes in these parameters. The sensitivity with respect to slider length is much smaller. This is expected, since slider length can only affect the normal force at the joint interface, which indirectly impacts the slider velocity due to change of friction characteristics. In contrast, change of link lengths will have a more direct effect on the slider velocity. The sensitivity with respect to slider width is zero and hence it has not been shown. This is due to the universal joint being located at the translational axis of the slider, and the torque produce about this axis is essentially zero. Hence, there is no change in the normal force due to a change in slider width.

Coming to sensitivities with respect to friction, the highest effect is observed due to changes in the dynamic friction coefficient μ_d. Naturally, this parameter has the highest influence on system dynamics since the time spent by the mechanism in stiction phase of friction is negligible in comparison to the time spent in sliding phase. The most interesting influence of friction on sensitivities, is that it adds 'discontinuity' or 'jumps' to an otherwise smooth solution observed for the frictionless model. The Brown McPhee friction model is C^1 continuous, however the transition phase from static to dynamic friction is very short lived. Hence there are sudden changes in sensitivities when the friction transitions to and from the static and dynamic phases. This can be verified by matching timestamps across the dynamics

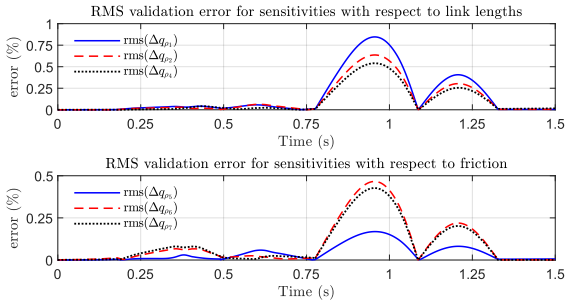

Fig. 12: Percent RMS validation error.

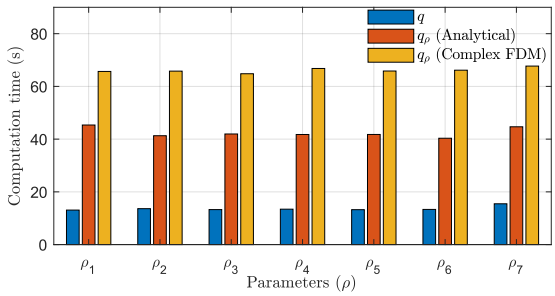

Fig. 13: Comparison of computational cost.

and sensitivity plots.

Now that the sensitivities have been computed using the analytical method, it is of crucial importance that these sensitivities are verified prior to applying the methodology for optimization problems. Incorrect model sensitivities might appear to satisfy the design objective of an optimization case study, but will fail to achieve the most optimal solution. Figure 12 shows the root mean squared deviation in position sensitivities with respect to complex finite differences. For this specific case study, the validation error was found to be less than 1% for all the design parameters. This is a positive indication for the methodology being capable of producing accurate sensitivities at a cheaper computational cost.

For a thorough assessment of computational efficiency, sensitivity methodologies need to be tested through programming in compiled languages like Fortran or C++. Moreover, online computation for all Jacobian matrices is not necessary, especially those taken with respect to generalized coordinates $\mathbf{q}$. Since the choice of design parameters can vary widely, for a completely general purpose code, online computation of Jacobian matrices taken with respect to design might be required. In such cases, Automatic Differentiation (AD) techniques [52,53] are much more efficient when compared to symbolic differentiation. In this work we get a baseline estimate of computational efficiency by comparing the solution times for dynamics, for analytical sensitivities, and for the complex FDM sensitivities, for different parameters values of the model. Results have been shown in Figure 13. These results were obtained for a simulation time of 1.5 seconds at a time step $h = 10^{-4}\,s$ and a convergence tolerance of 10^{-6}. This includes the online computation of all Jacobian matrices, which ranges from 25%-30% of the total computation time.

8 Conclusions

Through the case study it was observed that the dynamic response of the system for both Gonthier et al. and Brown McPhee friction models was very similar. There is certainly a trade-off associated with the choice of static friction models, including the Brown McPhee model, over dynamic ones. Some observations that were made during this study are as follows. Firstly, the Brown-McPhee model exhibits 'stiff' behavior at very low relative velocities. This may induce an incorrect temporal lag in the system and proper tuning of the transition velocity v_t might be required. Secondly, in the stiction experiment experiment, the Brown McPhee model does not demonstrate the 'decay' of excess energy which lead to gradually decreasing peaks in position and velocity plots until steady state values are reached. This phenomenon was an observation made by Rabinowicz [46] and is more noticeable as the sliding velocities increase. It can be modeled accurately using dwell-time dynamics in the Gonthier et al. model. Lastly, as noted before, the sensitivities with joint friction were similar to those typically observed in hybrid dynamic systems even though the model for the multibody system was smooth. This is a numerical artifact of the friction models, where the transition is abrupt, and the derivatives pick this transitions.

This concludes the work for direct sensitivity analysis of multibody systems with joint friction. As a future scope for this work, sensitivity methodologies can be developed using more robust and computationally efficient multibody formulations with joint friction. Also, since direct sensitivity approach is practical for problems involving high number of objective functions and a relatively small number of parameters, the adjoint sensitivity approach must be developed for systems with joint friction involving a large number of design parameters. Since the Brown McPhee model is a much simpler model, it is recommended to be used in applications that require real-time computations like design of control systems. Substantial work has gone into control of dynamical systems with friction [39, 54, 55]. Control strategies for multibody systems with Brown McPhee friction can be explored.

Acknowledgements

The work of C. Sandu has been supported in part by the Robert E. Hord Jr. professorship and by the Terramechanics, Multibody, and Vehicle Systems Laboratory at Virginia Tech. The work of A. Sandu has been supported in part by NSF through awards NSF ACI-1709727, NSF CDS&E-MSS 1953113, DOE ASCR DESC0021313, and by the Computational Science Laboratory at Virginia Tech. The work of D. Dopico was funded by the Spanish Ministry of Science and Innovation (MICINN) under project PID2020-120270GB-C21. The authors would also like to thank Prof. Ed Haug for his feedback on the current work.

REFERENCES

[1] Haug, E. J., and Arora, J. S., 1978. "Design sensitivity analysis of elastic mechanical systems". *Computer Methods in Applied Mechanics and Engineering,* **15**(1), Jul, pp. 35–62.

[2] Haug, E. J., Wehage, R. A., and Mani, N. K., 1984. "Design sensitivity analysis of large-scale constrained dynamic mechanical systems". *Journal of Mechanical Design, Transactions of the ASME,* **106**, pp. 156–162.

[3] Krishnaswami, P., and Bhatti, M., 1984. "A general approach for design sensitivity analysis of constrained dynamic systems". *ASME Journal of Mechanisms, Transmissions, and Automations in Design*, pp. 84–DET–132.

[4] Callejo, A., and Dopico, D., 2019. "Direct sensitivity analysis of multibody systems: A vehicle dynamics benchmark". *Journal of Computational and Nonlinear Dynamics,* **14**(2), pp. 1–9.

[5] Haug, E. J., 1987. "Design sensitivity analysis of dynamic systems". In Computer Aided Optimal Design: Structural and Mechanical Systems, C. A. Mota Soares, ed., Springer Berlin Heidelberg, pp. 705–755.

[6] Chang, C. O., and Nikravesh, P. E., 1985. "Optimal design of mechanical systems with constraint violation stabilization method". *Journal of Mechanisms, Transmissions, and Automation in Design,* **107**(4), Dec, pp. 493–498.

[7] Baumgarte, J., 1972. "Stabilization of constraints and integrals of motion in dynamical systems". *Computer Methods in Applied Mechanics and Engineering,* **1**(1), Jun, pp. 1–16.

[8] Pagalday, J. M., and Avello, A., 1997. "Optimization of multibody dynamics using object oriented programming and a mixed numerical-symbolic penalty formulation". *Mechanism and Machine Theory,* **32**(2), Feb, pp. 161–174.

[9] Dopico, D., Zhu, Y., Sandu, A., and Sandu, C., 2015. "Direct and adjoint sensitivity analysis of ordinary differential equation multibody formulations". *Journal of Computational and Nonlinear Dynamics*.

[10] Flores, P., Ambrósio, J., and Claro, J. P., 2004. "Dynamic analysis for planar multibody mechanical systems with lubricated joints". *Multibody System Dynamics,* **12**(1), pp. 47–74.

[11] Zhang, H., and Sandu, A., 2014. "Fatode: A library for forward, adjoint, and tangent linear integration of odes". *SIAM Journal on Scientific Computing,* **36**(5), pp. C504–C523.

[12] Corner, S., Sandu, C., and Sandu, A., 2019. "Modeling and sensitivity analysis methodology for hybrid dynamical system". *Nonlinear Analysis: Hybrid Systems,* **31**, pp. 19–40.

[13] Corner, S., Sandu, A., and Sandu, C., 2020. "Adjoint sensitivity analysis of hybrid multibody dynamical systems". *Multibody System Dynamics,* **49**(4), pp. 395–420.

[14] Blanchard, E., Sandu, A., and Sandu, C., 2009. "Parameter estimation for mechanical systems via an explicit representation of uncertainty". *Engineering Computations (Swansea, Wales),* **26**(5), pp. 541–569.

[15] Blanchard, E. D., Sandu, A., and Sandu, C., 2010. "A polynomial chaos-based kalman filter approach for parameter estimation of mechanical systems". *Journal of Dynamic Systems, Measurement and Control, Transactions of the ASME,* **132**(6), pp. 1–18.

[16] Blanchard, E. D., Sandu, A., and Sandu, C., 2010. "Polynomial chaos-based parameter estimation methods applied to a vehicle system". *Proceedings of the Institution of Mechanical Engineers, Part K: Journal of Multi-body Dynamics,* **224**(1), pp. 59–81.

[17] Flores, P., Ambrósio, J., Claro, J. C. P., and Lankarani, H. M., 2006. "Dynamics of Multibody Systems With Spherical Clearance Joints". *Journal of Computational and Nonlinear Dynamics,* **1**(3), 03, pp. 240–247.

[18] Orden, J. C. G., 2005. "Analysis of joint clearances in multibody systems". *Multibody System Dynamics,* **13**(4), May, pp. 401–420.

[19] Haug, E. J., Wu, S. C., and Yang, S. M., 1986. "Dynamics of mechanical systems with coulomb friction, stiction, impact and constraint addition-deletion—i theory". *Mechanism and Machine Theory,* **21**(5), pp. 401–406.

[20] Wu, S. C., Yang, S. M., and Haug, E. J., 1986. "Dynamics of mechanical systems with coulomb friction, stiction, impact and constraint addition-deletion—ii planar systems". *Mechanism and Machine Theory,* **21**(5), pp. 407–416.

[21] Wu, S. C., Yang, S. M., and Haug, E. J., 1986. "Dynamics of mechanical systems with coulomb friction, stiction, impact and constraint addition-deletion—iii spatial systems". *Mechanism and Machine Theory,* **21**(5), pp. 417–425.

[22] Synnestvedt, R. G., 1996. "An Effective Method for Modeling Stiction in Multibody Dynamic Systems". *Journal of Dynamic Systems, Measurement, and Control,* **118**(1), 03, pp. 172–176.

[23] Fraczek, J., and Wojtyra, M., 2011. "On the unique solvability of a direct dynamics problem for mechanisms with redundant constraints and Coulomb friction in joints". *Mechanism and Machine Theory,* **46**(3), pp. 312–334.

[24] Pennestrì, E., Valentini, P. P., and Vita, L., 2007. "Multibody dynamics simulation of planar linkages with Dahl friction". *Multibody System Dynamics,* **17**(4), pp. 321–347.

[25] Blumentals, A., Brogliato, B., and Bertails-Descoubes, F., 2016. "The contact problem in Lagrangian systems subject to bilateral and unilateral constraints, with or without sliding Coulomb's friction: a tutorial". *Multibody System Dynamics,* **38**(1), pp. 43–76.

[26] Wojtyra, M., 2017. "Modeling of static friction in closed-loop kinematic chains—Uniqueness and parametric sensitivity problems". *Multibody System Dynamics,* **39**(4), pp. 337–361.

[27] Harlecki, A., and Urbaś, A., 2017. "Modelling friction in the dynamics analysis of selected one-DOF spatial

linkage mechanisms". *Meccanica,* **52**(1-2), pp. 403–420.

[28] Haug, E. J., 2018. "Simulation of spatial multibody systems with friction". *Mechanics Based Design of Structures and Machines,* **46**(3), pp. 347–375.

[29] Brown, P., and McPhee, J., 2016. "A Continuous Velocity-Based Friction Model for Dynamics and Control with Physically Meaningful Parameters". *Journal of Computational and Nonlinear Dynamics,* **11**(5), pp. 1–6.

[30] Verulkar, A., Sandu, C., Dopico, D., and Sandu, A., 2021. "Direct sensitivity analysis of spatial multibody systems with joint friction using index-1 formulation". Vol. Volume 9: 17th International Conference on Multibody Systems, Nonlinear Dynamics, and Control (MSNDC) of *International Design Engineering Technical Conferences and Computers and Information in Engineering Conference*. V009T09A044.

[31] Gonthier, Y., McPhee, J., Lange, C., and Piedbœuf, J. C., 2004. "A regularized contact model with asymmetric damping and dwell-time dependent friction". *Multibody System Dynamics,* **11**(3), pp. 209–233.

[32] Zhu, Y., Dopico, D., Sandu, C., and Sandu, A., 2015. "Dynamic Response Optimization of Complex Multibody Systems in a Penalty Formulation Using Adjoint Sensitivity". *Journal of Computational and Nonlinear Dynamics,* **10**(3), pp. 1–9.

[33] Dopico, D., Sandu, A., and Sandu, C., 2021. "Adjoint sensitivity index-3 augmented lagrangian formulation with projections". *Mechanics Based Design of Structures and Machines,* **0**(0), pp. 1–31.

[34] Marques, F., Flores, P., Pimenta Claro, J. C., and Lankarani, H. M., 2016. "A survey and comparison of several friction force models for dynamic analysis of multibody mechanical systems". *Nonlinear Dynamics,* **86**(3), pp. 1407–1443.

[35] Berger, E. J., 2002. "Friction modeling for dynamic system simulation". *Applied Mechanics Reviews,* **55**(6), Nov., pp. 535–577.

[36] Cortes, J., 2008. "Discontinuous dynamical systems". *IEEE Control Systems Magazine,* **28**(3), pp. 36–73.

[37] Dahl, P., 1968. "A solid friction model". The Aerospace Corporation.

[38] Canudas de Wit, C., Olsson, H., Astrom, K., and Lischinsky, P., 1995. "A new model for control of systems with friction". *IEEE Transactions on Automatic Control,* **40**(3), pp. 419–425.

[39] Armstrong-Hélouvry, B., 1991. *Control of Machines with Friction*. Springer US, Boston, MA.

[40] Olsson, H., Åström, K., Canudas de Wit, C., Gäfvert, M., and Lischinsky, P., 1998. "Friction models and friction compensation". *European Journal of Control,* **4**(3), pp. 176–195.

[41] Bliman, P., and Sorine, M., 1995. "Easy-to-use realistic dry friction models for automatic control". In 3rd European Control Conference, Vol. 7, p. 3788–3794.

[42] Taylor, J. H., 1996. "Tools for Modeling and Simulation of Hybrid Systems – A Tutorial Guide". *University of New Brunswick*.

[43] Kikuuwe, R., Takesue, N., Sano, A., Mochiyama, H., and Fujimoto, H., 2005. "Fixed-step friction simulation: from classical coulomb model to modern continuous models". In 2005 IEEE/RSJ International Conference on Intelligent Robots and Systems, pp. 1009–1016.

[44] Karnopp, D., 1985. "Computer Simulation of Stick-Slip Friction in Mechanical Dynamic Systems". *Journal of Dynamic Systems, Measurement, and Control,* **107**(1), 03, pp. 100–103.

[45] Pennestrì, E., Rossi, V., Salvini, P., and Valentini, P. P., 2016. "Review and comparison of dry friction force models". *Nonlinear Dynamics,* **83**(4), pp. 1785–1801.

[46] Rabinowicz, E., 1961. "Stick and slip stick and slip". *American String Teacher,* **11**(2), pp. 18–20.

[47] Andersson, S., Söderberg, A., and Björklund, S., 2007. "Friction models for sliding dry, boundary and mixed lubricated contacts". *Tribology International,* **40**(4), pp. 580–587. NORDTRIB 2004.

[48] Specker, T., Buchholz, M., and Dietmayer, K., 2014. "A new approach of dynamic friction modelling for simulation and observation". *IFAC Proceedings Volumes,* **47**(3), pp. 4523–4528. 19th IFAC World Congress.

[49] Haug, E. J., 2016. "An Ordinary Differential Equation Formulation for Multibody Dynamics: Holonomic Constraints". *Journal of Computing and Information Science in Engineering,* **16**(2), 05. 021007.

[50] Dopico, D., Sandu, A., Sandu, C., and Zhu, Y., 2014. "Sensitivity analysis of multibody dynamic systems modeled by ODEs and DAEs". In Computational Methods in Applied Sciences.

[51] Haug, E. J., 1989. *Computer aided kinematics and dynamics of mechanical systems, volume 1: Basic methods*. Massachusetts.

[52] Callejo, A., 2013. "Dynamic response optimization of vehicles through efficient multibody formulations and automatic differentiation techniques.". PhD thesis, Universidad Politécnica de Madrid.

[53] Wang, S., Tian, Q., Hu, H., Shi, J., and Zeng, L., 2021. "Sensitivity analysis of deployable flexible space structures with a large number of design parameters". *Nonlinear Dynamics,* **105**(3), Aug, pp. 2055–2079.

[54] Armstrong-Hélouvry, B., Dupont, P., and De Wit, C. C., 1994. "A survey of models, analysis tools and compensation methods for the control of machines with friction". *Automatica,* **30**(7), pp. 1083–1138.

[55] Baril, C. G., 1993. Control of mechanical systems affected by friction and other nondifferentiable nonlinearities.